Macromolecules
ARTICLE

Macromolecules **2010**, *43*, 10297–10303 **10297**
DOI: 10.1021/ma102287v

Polyanhydride Networks from Thiol−Ene Polymerizations

Broden G. Rutherglen, Ryan A. McBath, Yu Ling Huang, and Devon A. Shipp*

Department of Chemistry and Biomolecular Science and Center for Advanced Materials Processing, Clarkson University, Potsdam, New York 13699-5810, United States

Received October 7, 2010; Revised Manuscript Received November 19, 2010

ABSTRACT: Thiol−ene photopolymerization was used in the synthesis of elastomeric polyanhydrides. Side reactions involving the addition of thiol to the anhydride were observed but take place at a much slower rate than photoinitiated thiol−ene polymerization. The thermomechanical properties, including the glass transition temperature (T_g) as well as tensile and compressive modulus, of the cross-linked material were studied using dynamic mechanical analysis. T_g values ranged from −15 to approximately −50 °C and were dependent on the degree of cross-linking. The Young's and compressive modulus measurements confirm that these types of networks are a soft rubber-like material at room and body temperature and become softer as the cross-linking density is reduced. The hydrophobicity/hydrophilicity of these networks was analyzed by water contact angle measurements. The polyanhydrides were moderately hydrophobic, with water contact angle averages ranging from 82° to 92°. This hydrophobicity, coupled with the high reactivity of the anhydride groups, results in the material eroding via the surface erosion mechanism.

Introduction

The most common class of polymer for degradable materials are polyesters, in particular poly(L-lactic acid), poly(glycolic acid), and poly(lactic-*co*-glycolic acid).[1,2] However, these polyesters lack many properties necessary for a variety of applications, especially in the medical arena, and undergo homogeneous bulk degradation, which is detrimental to the long-term mechanical properties of the material. Degradation rates can also be quite slow—from several months to years. Furthermore, their crystallinity leads to hard materials that deform upon degradation. In contrast, surface eroding polymers, such as polyanhydrides, maintain their mechanical integrity during degradation and exhibit a gradual loss in size.[3−5]

There are several polymer types that potentially can undergo surface erosion; these are typically those that are hydrophobic yet contain readily hydrolyzable groups. Notable examples are polyanhydrides and poly(orthoesters). Early work on poly(orthoesters) by Heller et al.[6] showed that these polymers undergo surface erosion and potentially can provide zero-order drug release kinetics. Such polymers are primarily made via the addition of polyols to diketene acetals.[7,8] However, degradation of poly(orthoesters) occurs only under acidic conditions. Polyanhydrides are the other major class of surface-eroding hydrophobic polymers. They were made by Hill and Carothers[9,10] as far back as the 1930s, but little more was done until the work of Conix[11] in the late 1950s and 1960s. The synthesis of early polyanhydrides was via a condensation of acetyl-protected diacids. Langer et al.[4,5,12−21] and others[22−31] have extensively studied these systems, and while many substructures were examined, copolyanhydrides based on sebacic acid (SA) and 1,3-bis(*p*-carboxyphenoxy)propane (CPP) proved to be quite successful and thus widely studied. One of the major results of this work was the development of the Gliadel Wafer for use as a drug delivery vehicle for combating brain cancer tumors; the Gliadel Wafer was FDA approved for this application in 1993.[32] Another advance in polyanhydrides was the development of methacrylated anhydrides which allow for the use of photoinitiation, providing fast curing rates, spatial and temporal control, and the ability to cure in vivo. These materials can be molded (e.g., into screws, in bone cavities, etc.) and have excellent mechanical strength that may be used in load-bearing devices.[15]

We have recently shown that polyanhydrides can be made using thiol−ene chemistry.[33] Thiol−ene polymerizations have been widely studied for several decades.[34−36] The polymerization occurs through radical intermediates and is unusual in that while a chain growth process (i.e., there are initiation, propagation, and termination steps) the development of the polymer molecular weight distribution is akin to a step-growth polymerization. A wide range of ene and thiols can be used to create network structures.[34,36] These cross-linked networks can have several advantages over those made by acrylic cross-linkers. For example, because of the step-growth process of molecular weight buildup, a much higher degree of cross-linking uniformity is obtained. This results in lower film stress, which improves adhesion to substrates. Furthermore, it also produces relatively narrow glass transitions. Thiol−ene polymerizations also display less shrinkage and very high monomer conversions.

The focus of this paper is to examine cross-linked polyanhydrides using photoinitiated thiol−ene polymerization, in particular to study their mechanical and physical characteristics and to tune these properties by altering the monomers used. Specifically, we report on potential side reactions between monomers, the behavior of physical and thermal properties on composition, such as the glass transition temperature, tensile and compression modulii, and hydrophobicity.

Experimental Section

Materials. All of the following materials were purchased from Sigma-Aldrich and were used as received after being characterized by ^{1}H NMR spectroscopy: 4-pentenoic anhydride (98%, PNA), pentaerythritol tetrakis(3-mercaptopropionate) (98%, PETMP), 3,6-dioxa-1,8-dithiooctane (95%, EGDT), valeric anhydride (97%, VA), 1-hydroxycyclohexyl phenyl ketone (99%).

*To whom correspondence should be addressed: Tel +1-315-268-2393; Fax +1-315-268-6610; e-mail dshipp@clarkson.edu.

Published on Web 12/06/2010

Scheme 1. Monomers Used for Thiol−Ene Polyanhydrides Synthesis and Outline of the Formation of Network Structures Based on 4-Pentenoic Anhydride/Pentaerythritol Tetrakis(3-mercaptopropionate) (PNA/PETMP) Monomers

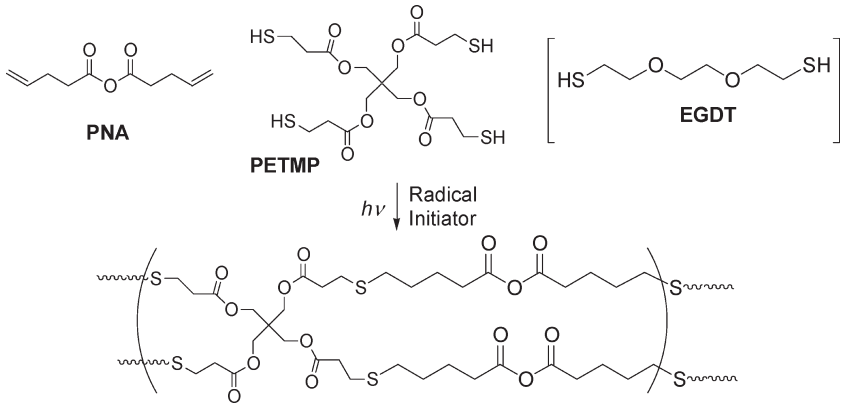

Instrumentation. ^{1}H (400 MHz) and ^{13}C (100 MHz) nuclear magnetic resonance (NMR) spectroscopy were performed on a Bruker Avance 400 with a BBO probe. The UV light source for curing was an Oriel Instruments, model 68811, 500 W mercury xenon arc lamp (intensity ~90 mW/cm^2, as measured by a Dymax Corp. Accu-Cal-30 intensity meter). Mechanical analyses were performed on a TA Instruments Q800 dynamic mechanical analyzer (DMA) equipped with a liquid nitrogen cooling accessory. Three different clamps that were provided with the instrument were used: single cantilever clamp (sample size: approximately 35 mm long, 15 mm wide, and 2 mm high), film tension clamp (sample size: 15 mm long, 5 mm wide, 0.6 mm high), and compression clamp (sample size: 15 mm diameter, 5 mm high). For single cantilever experiments, the samples were analyzed from −100 to 50 °C at a temperature ramp rate of 2 °C/min with a constant frequency of 1 Hz. For tensile measurements, the samples were examined isothermally at 37 °C and ramped at a force of 1 N/min to 18 N or until failure. For compression measurements, the samples were examined isothermally at 37 °C, and a ramp force rate of 1 N/min until the maximum of 18 N, and then ramped down from 18 to 0 N with the same ramp force rate. ATR-FTIR spectra were collected on a Bruker Vector 22 Infrared instrument equipped with Pike Technologies ATR apparatus with a MIRacle ZnSe crystal. Water contact angle measurements were performed on a KSV Instruments CAM-200 contact angle and surface tension meter equipped with computer software capable of surface and interfacial tension, static contact angles, and surface free energy of solids. The instrumentation includes a FireWire video camera, an adjustable sample stage, and a LED light source. All polymer compositions were tested three times, giving a total of six angles for each composition.

Example Procedure for the Synthesis of Cross-Linked Polyanhydrides. A typical procedure for the synthesis of the thiol−ene cross-linked polyanhydrides is as follows. 1-Hydroxycyclohexyl phenyl ketone (photoinitiator, 1.5 mg, 7.3×10^{-6} mol, 0.1 wt %) was weighed into a scintillation vial. PNA (0.768 mL, 0.0042 mol) was transferred using a micropipet into the vial, followed by PETMP (0.80 mL, 0.0021 mol). The mixture was then purged with N_2 gas for 3 min. The mixture was then transferred to a mold (Teflon or silicon rubber) and placed under the UV light for 15 min. After curing, the sample was removed from the mold and placed in a clean dry scintillation vial that was purged with N_2. Syntheses of samples containing EGDT were carried out similarly. Yield = 100%.

Example Procedure for the Study of Monomer Side Reactions. The EGDT (0.46 mL, 2.7 mmol) was transferred into a 15 mL round-bottom flask with either VA (0.54 mL, 2.7 mmol) or PNA (0.5 mL, 2.7 mmol). The flasks were stoppered with a rubber septum, purged with N_2 for 10 min, and then left at room temperature for 1 week. A small sample (~0.1 mL) was removed from the reaction flasks under an N_2 atmosphere and mixed with 1 mL of $CDCl_3$ for ^{1}H NMR analysis.

Results and Discussion

In our preliminary work,[33] we have shown that using commercially available monomers thiol−ene polymerization yields degradable polymers that, when cross-linked, appear to undergo surface erosion. Scheme 1 shows an outline of how thiol−ene polymerization yields cross-linked polyanhydrides. A diene anhydride and a tetrathiol, both of which are commercially available, were used in our preliminary experiments, and the same monomers are used to make the materials studied herein. In our initial communication we briefly examined the erosion behavior of these novel materials and did not explore their properties to any significant extent, nor did we study any possible side reactions that may occur during their synthesis. In this paper we undertake a more complete analysis of these side reactions and of the polyanhydride physical properties, primarily using dynamic mechanical analysis.

Given the high reactivity of the anhydride moiety, it is reasonable to expect that side reactions that may not lead to a cross-linked network might occur between monomers and/or adventitious water during the polymerization. Possible reactions that were studied include (1) thiol addition to the ene without initiator, (2) thioester formation from thiol addition to the anhydride, and (3) hydrolysis by adventitious water.

^{1}H NMR spectroscopy was used to determine if any of these reactions take place and if so to study their kinetics. Two different reaction conditions were studied: the first reaction included VA and EGDT (shown in the scheme above Figure 1) while the second reaction was between PNA and EGDT (shown in the scheme above Figure 2). The reaction between the VA, a model compound for PNA, and EGDT is expected to provide information regarding the reactivity of the thiol toward the anhydride, while the reaction with PNA and EGDT should also provide information about the possible addition of thiols to enes in the absence of photoinitiator. Such reactions may occur in the presence of light and/or oxygen that generate low concentrations of radicals. Both reactions can provide details about the hydrolysis of the anhydride with adventitious water. Both reactions were performed neat (no solvent) over several days at room temperature with no added photoinitiator. The reaction contents (VA and EDGT for reaction 1, PNA and EGDT for reaction 2) were placed in a round-bottom flask and purged with N_2 gas for 3 min. Small aliquots were taken daily and diluted with $CDCl_3$ for NMR analysis. All following assignments were based on analysis of ^{1}H NMR spectra from model compounds.

Figure 1 shows selected ^{1}H NMR spectra of reaction 1 from days 1−7. The peaks of particular interest are between 2.3 and 3.2 ppm, and each is labeled according to the assignments as given in the structures within the figure (letter labels are reactants, number labels are products). The peaks labeled **1**, **2**, and **3** at

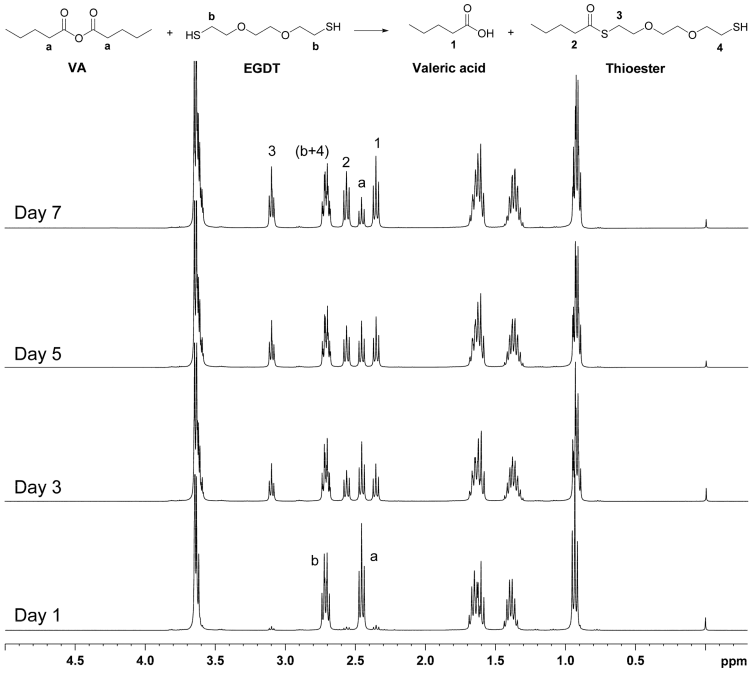

Figure 1. Select ^{1}H NMR spectra obtained from reaction between valeric anhydride (VA) and 3,6-dioxa-1,8-dithiooctane (EGDT) (reaction 1).

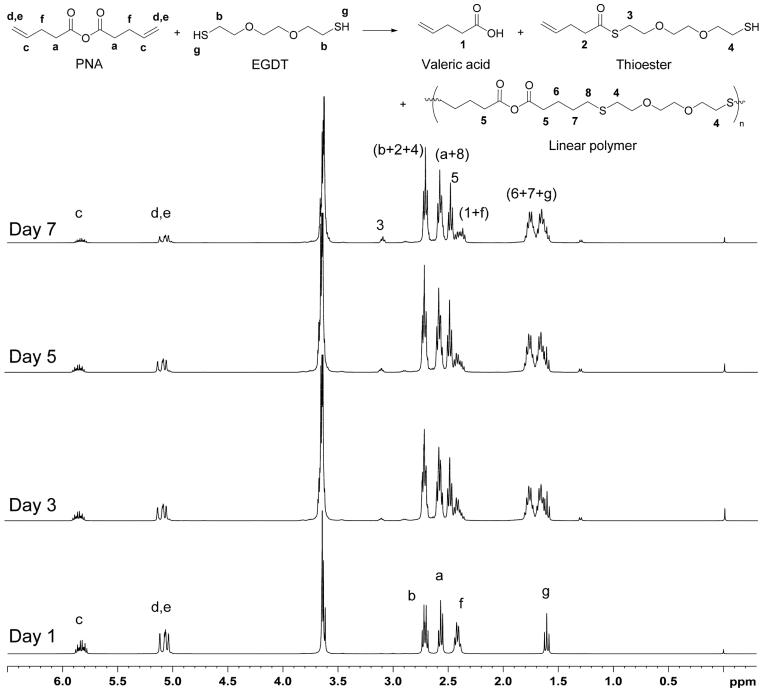

Figure 2. Select ^{1}H NMR spectra obtained from reaction between 4-pentenoic anhydride (PNA) and 3,6-dioxa-1,8-dithiooctane (EGDT) (reaction 2).

~2.35, ~2.55, and ~3.1 ppm correspond to protons within the thioester and valeric acid. At the beginning of the reaction, the peaks from the thioester and valeric acid are hardly observable, but after 7 days these peaks become quite prominent. This data provides evidence that thiols undergo nucleophilic acyl substitution with the anhydride, albeit slowly compared with the time frame of the photoinitiated polymerizations studied here.

In Figure 2 are select ^{1}H NMR spectra taken for reaction 2 between days 1 and 7, along with a depiction of the monomers and products expected to form from reaction of the anhydride with the thiol (thioester formation) and the thiol and the ene (which would result in polymerization). The peaks of interest have been labeled, along with the corresponding protons on the scheme within the figure. In addition to the appearance of peaks due to thioester and carboxylic acid formation (as discussed above for the VA + EGDT reaction), the most important aspect of this reaction is that the signals from the vinyl (~5−5.1 and 5.8−5.9 ppm) and thiol (~1.6 ppm) groups decrease by day 7. This is evidence that, even without photoinitiator included in the reaction, the thiol still adds across the alkene, although slowly. The spectra also show that the linear polymer has formed. This can be concluded by comparing the spectra from our earlier work[33] with Figure 2. Furthermore, it is also evident that thiol addition to the ene occurs faster than the thiol−anhydride reaction. This can be seen from the relative sizes of peaks **3**

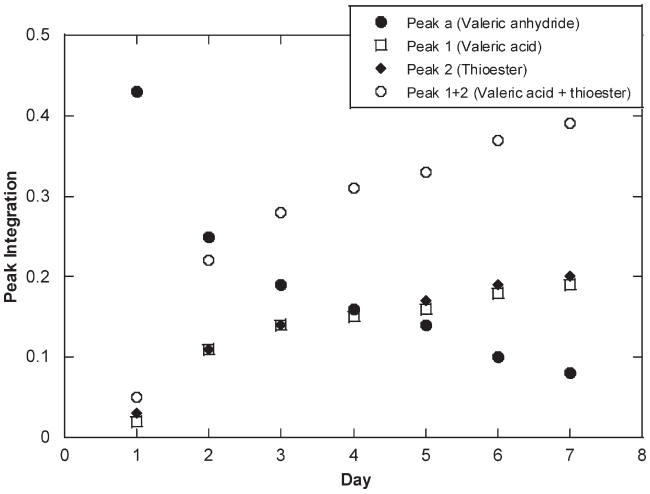

Figure 3. Plot of the integration values versus days for peaks **a**, **1**, **2**, and the sum of peaks (**1** + **2**) from the ^{1}H NMR spectra obtained from reaction between valeric anhydride (VA) and 3,6-dioxa-1,8-dithiooctane (EGDT) (reaction 1).

(from the valeric acid, a product of thioester formation) and peak **5** (due to polymerization) or peaks (**6** + **7**), for example.

Kinetic evaluation of these spectra further justifies our conclusion that the thiol adds to both the anhydride and ene groups, but over a time frame that is much longer than what the photoinitiated polymerizations were conducted. Shown in Figure 3 are the relative integration values of peaks due to protons **a**, **1**, and **2** in the spectra taken of reaction 1 (VA + EGDT). It can be clearly seen in this plot that as the reaction proceeds the integration values of the α-protons from the anhydride (peak **a**) decreases at the same rate as the increase in the sum of the integration values of the valeric acid and thioester (labeled peaks **1** and **2**), which as expected show a 1:1 ratio when compared with each other. This trend is expected if the reaction between anhydride and thiol occurs stoichiometrically and only forms the valeric acid and thioester. Similarly, a plot of the integration values of peak **4** and (**5** + **d**), corresponding to protons that are attached to the carbons adjacent to the thiol groups, also show a correlation (see Supporting Information Figure S1).

The other potential side reaction of concern was hydrolysis of the anhydride with adventitious water. While this would not necessarily lead to problems with the polymerization, it would obviously reduce the degree of cross-linking in the material and thus deleteriously affect properties. However, on the basis of the data shown in Figures 1−4, it can be concluded that this reaction is not significant. This conclusion is reached because as shown in Figure 3, peak **1** in Figure 1 (due to the α-protons on the acid) increases at the same rate as peak **2** (the α-protons on the thioester). If the hydrolysis reaction had occurred, the integration values of peak **1** should be larger than integration values of peak **2**.

In any cross-linked materials, the physical and thermal properties may be significantly affected by small molecule additives (e.g., plasticizers) or indeed unreacted monomer. In the present case, it is well-known that thiol−ene polymerizations often reach very high (≫90%) conversions.[34] However, it is necessary to ensure that no small molecule impurities, i.e., monomer, are present in the samples before mechanical and thermal analysis. Hence, cross-linked polyanhydrides samples of each of the four compositions shown in Table 1 were synthesized and examined by ATR-FTIR. Figure 4 shows the resulting ATR-FTIR spectra of cured materials after they had been sectioned. The peaks of interest are those due to the alkene and thiol functionalities; these should occur at ∼1640−1650 and 2565 cm^{-1}, respectively. The spectra clearly show the absence of the thiol peaks and very little, if any,

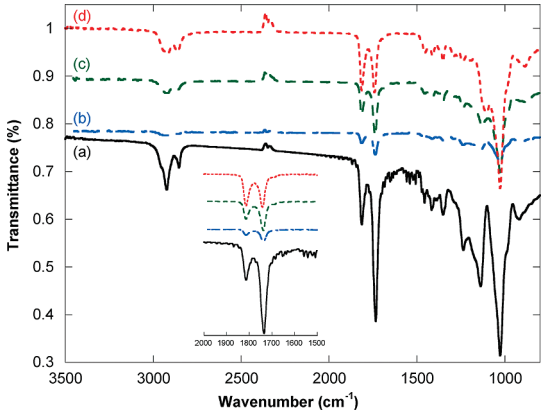

Figure 4. ATR-FTIR spectra of thiol−ene polyanhydride films (reactions 3−6, Table 1). Spectra are offset (*y*-axis) for clarity. 4-Pentenoic anhydride:pentaerythritol tetrakis(3-mercaptopropionate):3,6-dioxa-1,8-dithiooctane (PNA:PETMP:EGDT) functional group ratios (a) 1:1:0, (b) 1:0.75:0.25, (c) 1:0.50:0.50, and (d) 1:0.25:0.75.

indication of alkene peaks. The reason why there is a small amount of alkenes after the polymerization while no thiol remains, even though they are used in a 1:1 stoichiometry in all reactions, is that a small amount of the thiol undergoes reaction with the anhydride, thus creating a slight stiochiometric imbalance and leaving some alkene groups unreacted (vide supra). Hence, on the basis of the IR data (see inset in Figure 4) and preliminary ^{1}H NMR data of the degradation product which shows some vinyl protons present (particularly for the PNA/PETMP system, i.e., reaction 3 in Table 1), we conclude that essentially 100% of the thiol monomer functionality and approximately >95% of alkene functionality have been reacted. Also of note in the spectra are the presence of the characteristic dual peaks of the anhydride at ∼1730−1740 and ∼1815 cm^{-1}.

Evaluation of the relative hydrophobicities of the polyanhydride networks was undertaken by measurement of water contact angles. This was done because hydrophobicity is a factor that influences the degradation rates, and it is well-known that surface erosion is more likely with hydrophobic materials.[5] Three separate measurements for each of the four compositions were taken and averaged. These results are displayed in Table 1. The samples are moderately hydrophobic, with contact angles ranging from 82° to 92°, and surprisingly have no clear trend appearing based on the composition. This may be due to the PETMP preferentially locating at the surface prior to curing (at the expense of the hydrophilic EDGT), and once cured the surface hydrophobicity all appear to be similar. Water contact angles of similar types of material are typically in a comparable range. For example, poly(anhydride esters) give contact angles in the range of 75°−95°; one such material is poly(1,8-bis(*o*-carboxyphenoxy)octanoate) which gave a contact angle of 87°.[22] The contact angle for poly(SA) is 60°−64°,[37] and thiol−ene hydrogels, formed from poly(ethylene glycol) using an ester based triazine trithiol cured with a diallylic poly(ethylene glycol), has been measured to have a contact angles of 60°−80°.[38]

Each of the four compositions of cross-linked polyanhydrides was tested by dynamic mechanical analysis (DMA). The glass transition temperatures (T_g) were determined at the maximum of the tan δ curves. Five to seven samples of each polymer were heated from −100 to 50 °C at a ramp rate of 2 °C/min and a constant frequency of 1 Hz using the single cantilever clamp on the DMA. Representative modulus (E') and tan δ curves are given in Figures 5 and 6, respectively. The values for averaged rubbery E' (at T_g + 20 °C) and the T_g are summarized in Table 1.

Table 1. Synthetic Details and Physical Properties of Cross-Linked Polyanhydrides Made by Thiol−Ene Polymerization[a]

system	functional group ratio[b]	T_g (°C)	tan δ fwhm (°C)	E' at (T_g + 20 °C) (MPa)	ρ_x (M)	water contact angle (deg)	Young's modulus[c] (MPa)
reaction 3	1:1:0	−15	9.7	6.29	0.91	85 ± 5	10.2 ± 1.1
reaction 4	1:0.75:0.25	−28	14.8	4.36	0.66	92 ± 6	9.0 ± 0.9
reaction 5	1:0.5:0.5	−38	13.9	3.90	0.61	85 ± 4	8.1 ± 0.7
reaction 6	1:0.25:0.75	−55	11.5	3.27	0.55	82 ± 7	4.3 ± 0.4

[a] Glass transition temperature (T_g), width of tan δ (expressed as full width at half-maximum), elastic modulus (E'), cross-link density (ρ_x), water contact angle, and Young's modulus. [b] 4-Pentenoic anhydride:pentaerythritol tetrakis(3-mercaptopropionate):3,6-dioxa-1,8-dithiooctane (PNA:PETMP:EGDT). [c] Determined at 37 °C.

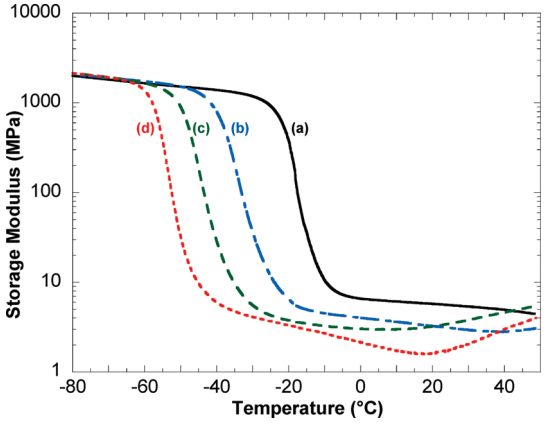

Figure 5. Storage modulus as a function of temperature of thiol−ene polyanhydride films (reactions 3−6, Table 1). 4-Pentenoic anhydride: pentaerythritol tetrakis(3-mercaptopropionate):3,6-dioxa-1,8-dithiooctane (PNA:PETMP:EGDT) functional group ratios (a) 1:1:0, (b) 1:0.75:0.25, (c) 1:0.50:0.50, and (d) 1:0.25:0.75.

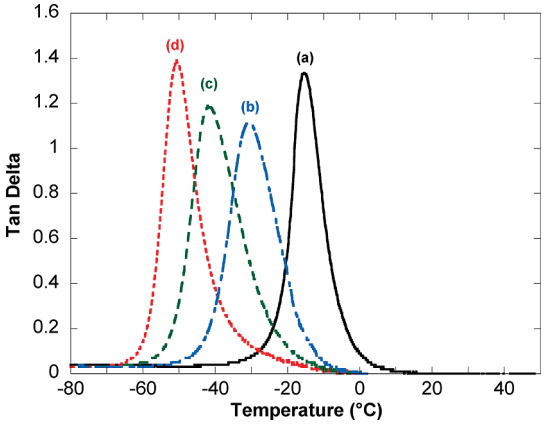

Figure 6. Tan δ curves, with T_g values as indicated in the figure, of thiol−ene polyanhydride films (reactions 3−6, Table 1). 4-Pentenoic anhydride: pentaerythritol tetrakis(3-mercaptopropionate):3,6-dioxa-1,8-dithiooctane (PNA:PETMP:EGDT) functional group ratios (a) 1:1:0, (b) 1:0.75:0.25, (c) 1:0.50:0.50, and (d) 1:0.25:0.75.

The T_g values range from approximately −15 °C to approximately −50 °C, with a direct relationship between the T_g and the amount of EGDT that is present in the polymer: i.e., as the amount of EGDT is increased, the T_g drops by roughly 11−14 °C for each 25% increase in EGDT. This lowering of T_g is due to the decrease in cross-linked density. This is in agreement with observations by Hoyle et al. that the more thiol groups that are incorporated in a given polymer, the lower the T_g will become.[34] The thiol−ene T_g data are comparable to thiol−acrylate systems, such as the study by Clarke et al.[39] where the T_g for a tetrathiol−diacrylate system (PETMP:HDDA (1,6-hexanediol diacrylate)) was found to be −15.4 °C. Polyanhydrides, such as poly(CPH), are reported to have T_g's of 47 °C and become a lot lower (about 7−8 °C) when an ethylene glycol based monomer (1,8-bis(*p*-carboxyphenoxy)-3,6-dioxaoctane) is added.[30] This qualitatively agrees with our observation that as the EGDT is added to polyanhydride matrix, the T_g's are decreased. Another important aspect is the sharpness of the tan δ peaks; such a characteristic is an indication of the homogeneity in the cross-linking network. In the thiol−ene polyanhydrides materials presented here, the tan δ peaks are quite narrow, 10−15 °C at full width at half-maximum. Narrow tan δ peaks are often observed in thiol−ene network structures and are often much narrower compared to acrylic cross-linked networks.[34]

The cross-link density (ρ_x) can also be determined from the elastic modulus (E') obtained from DMA measurements. Both parameters are presented in Table 1. The modulus at 20 °C above the T_g ranges from 3.3 to 6.3 MPa, indicating the elastic nature of the materials at these temperatures. In the glass region, the modulus for each sample ranged in the hundreds of MPa. The cross-link density was determined by analyzing the rubbery regime of the elastic modulus in a manner similar to Fairbanks et al.[40] using eq 1.

$$\rho_x = E'/([2(1+\nu)]RT) \quad (1)$$

Here, ν is Poisson's ratio (= 0.5 assuming an incompressible system), R is the gas constant, T is the temperature, and E' is the elastic modulus. The cross-link density (ρ_x) values for the samples shown in Table 1 are similar to those previously determined for cross-linked thiol−ene networks. As expected, the cross-link density decreases as the amount of EGDT increases (and PETMP decreases).

DMA was also used to evaluate the Young's modulus of the four compositions. Samples of the four formulations were analyzed isothermally at 37 °C, in order to mimic physiological temperature, and then subjected to a force from 0 to 18 N (or until failure) at a ramp rate of 1 N/min. Four or five replicates of each sample were analyzed within a few hours of synthesis. The results for these experiments can be found in the Supporting Information (Figures S2−S5). The data show that as the amount of EGDT is increased, thus decreasing the cross-linking density of the polymer, the tensile strength of the polymers is reduced. Young's modulus data were calculated from the initial slopes of these stress−strain curves (up to 6% strain) and are given in Table 1. The highest Young's modulus is obtained from the polymer composition with no EGDT (10.2 MPa) and the lowest obtained from the 75% EGDT polymer (4.3 MPa). Thus, the thiol−ene polyanhydrides display tensile properties typical to that of rubbery materials.

Compressive measurements were also conducted to further examine the mechanical properties of the four polymers. The samples were again examined isothermally at 37 °C within a few hours of synthesis, with a ramp force of 1 N/min until the maximum of 18 N, and then ramped back to 0 from 18 N also at 1 N/min. Data obtained from three of the four compositions of polymer are shown below in Figure 7. As would be expected, as the percentage of EGDT is increased the strain % of the polymers also increases. The sample with the largest amount of EGDT completely deformed after the compression. Again, these results

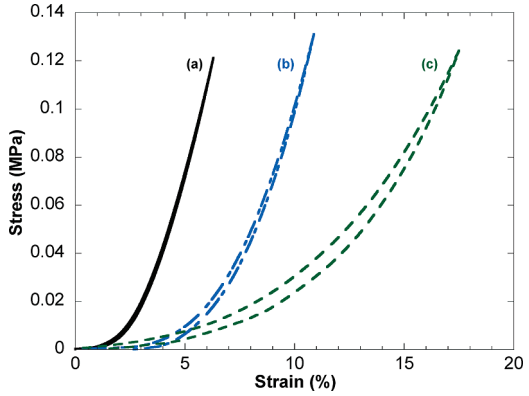

Figure 7. Compressive stress−strain plots of polyanhydrides made by thiol−ene polymerizations (reactions 3−5, Table 1). 4-Pentenoic anhydride:pentaerythritol tetrakis(3-mercaptopropionate):3,6-dioxa-1,8-dithiooctane (PNA:PETMP:EGDT) functional group ratios (a) 1:1:0, (b) 1:0.75:0.25, and (c) 1:0.50:0.50.

can be related to the higher rigidity and cross-link density in samples containing less EGDT. Also, greater hysteresis is observed in samples with more EGDT, an indication of the elasticity and deformation resistance of samples with less (no) EGDT. The 75% EGDT sample failed most likely due to the very low cross-link density and the soft, adhesive properties at 37 °C.

Conclusions

The synthesis, via thiol−ene polymerization, and physical and thermal characterization of photoinitiated cross-linked degradable polyanhydrides were carried out. The addition of thiol to the anhydride was observed but takes place at a much slower rate than photoinitiated thiol−ene polymerization. However, in polymerizations using a stoichiometric amount of thiol and ene, this side reaction results in a slight excess of ene functionality. The thermomechanical properties, including the glass transition temperature (T_g) as well as tensile and compressive modulus, of the cross-linked material were studied using DMA. The T_g values ranged from −15 to approximately −50 °C. As often seen in thiol−ene cross-linked networks, the tan δ peaks appeared quite narrow. The Young's and compressive modulus measurements confirm that these types of networks are a soft rubber-like material and become softer as the cross-linking density is reduced. The hydrophobicity/hydrophilicity of these networks was analyzed by contact angle measurements. The four compositions of polyanhydrides studied possess surfaces that are moderately hydrophobic, with contact angle averages ranging from approximately 82° to 92°. These results are similar to previously studied polyanhydrides which were also found to be hydrophobic materials.

This work demonstrates that thiol−ene polymerization can be used to produce cross-linked anhydride-containing materials that have been previously shown to undergo the oft-preferred surface-eroding characteristic. The step growth mechanism involved with thiol−ene polymerization allows for the possibility of a variety of thiol and ene monomers to be used in combination, thus giving the freedom to tune the rates and properties of the final material in order to suit many applications. Because of the elastic and adhesive-like characteristics of the polymers studied here, some applications for these thiol−ene/polyanhydrides could be in controlled drug delivery, tissues adhesives, and wound closure.

Acknowledgment. We thank the Department of Chemistry and Biomolecular Science at Clarkson University, the Center for Advanced Materials Processing at Clarkson University, a New York State Center for Advanced Technology, the GK-12 Project-Based Learning Partnership Program at Clarkson University, funded by the NSF (Program # DGE-0338216), and the McNair Program at Clarkson University for financial support. We also thank the US Army Research Office for a DURIP grant (#W911NF-08-1-0524) for funding the purchase of a DMA.

Supporting Information Available: Plot of integration values for ^{1}H NMR spectra and plots of DMA tensile data for PNA/PETMP/EGDT polyanhydrides networks. This material is available free of charge via the Internet at http://pubs.acs.org.

References and Notes

(1) Duncan, R.; Ringsdorf, H.; Satchi-Fainaro, R. *Adv. Polym. Sci.* **2006**, *192*, 1–8.
(2) Finne-Wistrand, A.; Albertsson, A.-C. *Annu. Rev. Mater. Res.* **2006**, *36*, 369–395.
(3) Göpferich, A.; Tessmar, J. *Adv. Drug Delivery Rev.* **2002**, *54*, 911–931.
(4) Katti, D. S.; Lakshmi, S.; Langer, R.; Laurencin, C. T. *Adv. Drug Delivery Rev.* **2002**, *54*, 933–961.
(5) Kumar, N.; Langer, R.; Domb, A. J. *Adv. Drug Delivery Rev.* **2002**, *54*, 889–910.
(6) Heller, J. *Biomaterials* **1990**, *11*, 659–665.
(7) Heller, J.; Barr, J. *Biomacromolecules* **2004**, *5*, 1625–1632.
(8) Heller, J.; Barr, J.; Ng, S. Y.; Schwach-Abdellauoi, K.; Gurny, R. *Adv. Drug. Delivery Rev.* **2002**, *54*, 1015–1039.
(9) Hill, J. W. *J. Am. Chem. Soc.* **1930**, *52*, 4110–4114.
(10) Hill, J. W.; Carothers, W. H. *J. Am. Chem. Soc.* **1932**, *54*, 1569–1579.
(11) Conix, A. In *Macromolecular Syntheses*; Wiley: New York, 1963; Vol. *2*, pp 95−99.
(12) Tarcha, P. J.; Su, L.; Baker, T.; Langridge, D.; Shastri, V.; Langer, R. *J. Polym. Sci., Part A: Polym. Chem.* **2001**, *39*, 4189–4195.
(13) Langer, R. *Acc. Chem. Res.* **2000**, *33*, 94–101.
(14) Uhrich, K. E.; Cannizzaro, S. M.; Langer, R.; Shakesheff, K. M. *Chem. Rev.* **1999**, *99*, 3181–3198.
(15) Anseth, K. S.; Shastri, V. R.; Langer, R. *Nature Biotechnol.* **1999**, *17*, 156–159.
(16) Gao, J.; Niklason, L.; Zhao, X.-M.; Langer, R. *J. Pharm. Sci.* **1998**, *87*, 246–248.
(17) Uhrich, K. E.; Gupta, A.; Thomas, T. T.; Laurencin, C. T.; Langer, R. *Macromolecules* **1995**, *28*, 2184–2193.
(18) Tamada, J. A.; Langer, R. *Proc. Natl. Acad. Sci. U.S.A.* **1993**, *90*, 552–556.
(19) Domb, A. J.; Mathiowitz, E.; Ron, E.; Giannos, S.; Langer, R. *J. Polym. Sci., Part A: Polym. Chem.* **1990**, *29*, 571–579.
(20) Domb, A. J.; Langer, R. *J. Polym. Sci., Part A: Polym. Chem.* **1987**, *25*, 3373–3386.
(21) Shieh, L.; Tamada, J.; Chen, I.; Pang, J.; Domb, A.; Langer, R. *J. Biomed. Mater. Res.* **1994**, *28*, 1465–1475.
(22) Prudencio, A.; Schmeltzer, R. C.; Uhrich, K. E. *Macromolecules* **2005**, *38*, 6895–6901.
(23) Ben-Shabat, S.; Abuganima, E.; Raziel, A.; Domb, A. J. *J. Polym. Sci., Part A: Polym. Chem.* **2003**, *41*, 3781–3787.
(24) Teomim, D.; Domb, A. J. *Biomacromolecules* **2001**, *2*, 37–44.
(25) Determan, A. S.; Graham, J. R.; Pfeiffer, K. A.; Narasimhan, B. *J. Microencapsulation* **2006**, *23*, 832–843.
(26) Kipper, M. J.; Narasimhan, B. *Macromolecules* **2005**, *38*, 1989–1999.
(27) Kipper, M. J.; Wilson, J. H.; Wannemuehler, M. J.; Narasimhan, B. *J. Biomed. Mater. Res., Part A* **2006**, *76A*, 798–810.
(28) Lopac, S. K.; Torres, M. P.; Wilson-Welder, J. H.; Wannemuehler, M. J.; Narasimhan, B. *J. Biomed. Mater. Res., Part B* **2009**, *91B*, 938–947.
(29) Torres, M. P.; Determan, A. S.; Anderson, G. L.; Mallapragada, S. K.; Narasimhan, B. *Biomaterials* **2007**, *28*, 108–116.
(30) Torres, M. P.; Vogel, B. M.; Narasimhan, B.; Mallapragada, S. K. *J. Biomed. Mater. Res., Part A* **2006**, *76A*, 102–110.
(31) Ulery, B. D.; Phanse, Y.; Sinha, A.; Wannemuehler, M. J.; Narasimhan, B.; Bellaire, B. H. *Pharm. Res.* **2009**, *26*, 683–690.
(32) Brem, H.; Piantadosi, S.; Burger, P. C.; Walker, M.; Selker, R.; Vick, N. A.; Black, K.; Sisti, M.; Brem, S.; Mohr, G.; Muller, P.; Morawetz, R. *Lancet* **1995**, *345*, 1008–1012.
(33) Shipp, D. A.; McQuinn, C. W.; Rutherglen, B. G.; McBath, R. A. *Chem. Commun.* **2009**, 6415–6417.

(34) Hoyle, C. E.; Lee, T. Y.; Roper, T. *J. Polym. Sci., Part A: Polym. Chem.* **2004**, *42*, 5301–5338.
(35) Hoyle, C. E.; Bowman, C. N. *Angew. Chem., Int. Ed.* **2010**, *49*, 1540–1573.
(36) Hoyle, C. E.; Lowe, A. B.; Bowman, C. N. *Chem. Soc. Rev.* **2010**, *39*, 1355–1387.
(37) Chickering, D. E., III; Jacob, J. S.; Mathiowitz, E. *React. Polym.* **1995**, *25*, 189–206.
(38) Lundberg, P.; Bruin, A.; Klijnstra, J. W.; Nystrm, A. M.; Johansson, M.; Malkoch, M.; Hult, A. *ACS Appl. Mater. Interfaces* **2010**, *2*, 903–912.
(39) Clark, T.; Kwisnek, L.; Hoyle, C. E.; Nazarenko, S. *J. Polym. Sci., Part A: Polym. Chem.* **2009**, *47*, 14–24.
(40) Fairbanks, B. D.; Scott, T. F.; Kloxin, C. J.; Anseth, K. S.; Bowman, C. N. *Macromolecules* **2009**, *42*, 211–217.